

# DECENTRALIZED $\mathcal{H}_2$ CONTROL FOR CIVIL STRUCTURES THROUGH HOMOTOPIC TRANSFORMATION

Yang Wang

*Georgia Institute of Technology, Atlanta, GA 30332, USA*

[yang.wang@ce.gatech.edu](mailto:yang.wang@ce.gatech.edu)

Kincho H. Law

*Stanford University, Stanford, CA 94305, USA*

[law@stanford.edu](mailto:law@stanford.edu)

Chin-Hsiung Loh

*National Taiwan University, Taipei 106, Taiwan*

[loh0220@ntu.edu.tw](mailto:loh0220@ntu.edu.tw)

## Abstract

As control devices are becoming smaller, more cost effective, and more reliable, opportunities are now available to instrument a structure with large number of control devices. With densely installed sensing and control devices, scalability of control systems will be hindered by their dependence on centralized control strategies. This paper presents a time-delayed decentralized  $\mathcal{H}_2$  output feedback controller design for large-scale feedback structural control. In a decentralized control system, control decisions can be made based upon data acquired only from sensors located in the vicinity of a control device. The decentralized  $\mathcal{H}_2$  controller design is achieved through homotopic transformation. Linear matrix inequality (LMI) constraints are ensured in the homotopic search, so that the  $\mathcal{H}_2$  control criteria are satisfied. The proposed algorithm is validated through numerical simulations with a five-story example structure. Performance of the proposed  $\mathcal{H}_2$  controller design is compared with a decentralized  $\mathcal{H}_\infty$  controller design, as well as with a time-delayed decentralized controller design that is based upon the linear quadratic regulator (LQR) criteria.

## Introduction

Utilizing a network of sensors, controllers and control devices, feedback control systems can potentially mitigate excessive dynamic responses of a structure subjected to strong dynamic loads, such as earthquakes or typhoons (Housner *et al.* 1997). As control devices are becoming smaller, more cost effective and reliable, opportunities are now available to instrument a structure with large number of control devices (Spencer and Nagarajaiah 2003). With densely installed sensing and control devices, scalability of control systems will be hindered by their dependence on centralized control strategies, where a central controller is responsible for acquiring data and making control decisions. To mitigate some of the difficulties with centralized feedback control systems, decentralized control strategies can be explored (Sandell *et al.* 1978; Siljak 1991). In a decentralized control system, distributed controllers can be designed to make control decisions using only neighborhood sensor data, and to command control devices only in the vicinity area.

Some early research on decentralized structural control focused on applications in cable-stayed bridges. A majority of the studies treated the interactions between subsystems or substructures as unknown disturbances; therefore, individual decentralized controllers aim to improve local control performance and cannot take global optimality into consideration (Cao *et al.* 2000; Luo *et al.* 2002; Volz *et al.* 1994). With the focus shifted to building control, Lynch and Law (2002; 2004) proposed market-based structural control strategies that model a structural control system as a competitive market. Following rules of a free market, distributed sellers and buyers reach the optimal allocation of limited control energy. Wang *et al.* (2007) described a decentralized static output feedback control strategy that is based upon the linear quadratic regulator (LQR) criteria. Sparsity shape constraints upon the gain matrices are employed to represent decentralized feedback patterns; iterative gradient searching is adopted for computing

decentralized gain matrices that optimize the control performance over the entire structure. By dividing a large structure into multiple substructures, Loh and Chang (2008) conducted analytical study of decentralized control approaches that apply linear quadratic Gaussian method to individual substructures. In addition, Lu, Loh, Yang and Lin (2008) studied the performance of fully decentralized sliding mode control algorithms; the algorithms require only the stroke velocity and displacement of a control device to make the control decision for the device. For structural systems that are instrumented with collocated rate sensors and actuators, Hiramoto and Grigoriadis (2008) explored decentralized static feedback controller design in continuous-time domain. More recently, Swartz and Lynch (2009) presented a partially decentralized linear quadratic regulation control scheme that employs redundant state estimation as a means of minimizing the need for the communication of data between sensors.

The authors' have previously explored time-delayed decentralized  $\mathcal{H}_\infty$  controller design (Wang 2010; Wang *et al.* 2009). The decentralized controller design employs a homotopy method that gradually transforms a centralized controller into multiple decentralized controllers. Linear matrix inequality constraints are included in the homotopic transformation to ensure optimal control performance. The approach adapts the homotopy method described by Zhai, *et al.* (2001), where the method was originally developed for designing decentralized  $\mathcal{H}_\infty$  controllers in continuous-time domain. Homotopy approaches for decentralized  $\mathcal{H}_\infty$  control in continuous-time domain have also been explored by Mehendale and Grigoriadis (2008).

This paper presents a time-delayed decentralized structural control strategy that aims to minimize the  $\mathcal{H}_2$  norm of the closed-loop system. Centralized  $\mathcal{H}_2$  controller design for structural control has been studied by many researchers, through both laboratory experiments and numerical simulations (Ankireddi and Yang 1999; Dyke *et al.* 1996; Johnson *et al.* 1998; Spencer *et al.* 1994; Yang *et al.* 2003). Their studies have shown the effectiveness of centralized  $\mathcal{H}_2$  control for civil structures. In contrast, this paper focuses on the time-delayed decentralized  $\mathcal{H}_2$  controller design. The paper first presents in detail a homotopy algorithm for computing decentralized  $\mathcal{H}_2$  controllers. A numerical example is provided to illustrate the performance of the time-delayed decentralized  $\mathcal{H}_2$  control algorithm. In addition, the results from the  $\mathcal{H}_2$  control design are compared to the decentralized  $\mathcal{H}_\infty$  and LQR controller designs and to assess the relative merits of the three time-delayed decentralized controller designs.

## Problem Formulation

The detailed description for the time-delayed decentralized control problem has been presented by Wang (2010). For completeness, the following briefly summarizes the formulation. For a structural model with  $n$  degrees-of-freedom (DOF) and instrumented with  $n_u$  control devices, the structural system and a system describing time-delay and sensor noise effect can be cascaded into following open-loop system:

$$\begin{cases} \mathbf{x}[k+1] = \mathbf{A}\mathbf{x}[k] + \mathbf{B}_1\mathbf{w}[k] + \mathbf{B}_2\mathbf{u}[k] \\ \mathbf{z}[k] = \mathbf{C}_1\mathbf{x}[k] + \mathbf{D}_{11}\mathbf{w}[k] + \mathbf{D}_{12}\mathbf{u}[k] \\ \mathbf{y}[k] = \mathbf{C}_2\mathbf{x}[k] + \mathbf{D}_{21}\mathbf{w}[k] + \mathbf{D}_{22}\mathbf{u}[k] \end{cases} \quad (1)$$

The system input  $\mathbf{w} = [\mathbf{w}_1^T \quad \mathbf{w}_2^T]^T \in \mathbb{R}^{n_w \times 1}$  contains both the external excitation  $\mathbf{w}_1$  and the sensor noise  $\mathbf{w}_2$ ,  $\mathbf{u} \in \mathbb{R}^{n_u \times 1}$  denotes the control force vector,  $\mathbf{x} \in \mathbb{R}^{n_{ol} \times 1}$  is the open-loop state vector, which contains the state vector of the structural system,  $\mathbf{x}_s \in \mathbb{R}^{2n \times 1}$ , and the state vector of the time-delay and sensor noise system,  $\mathbf{x}_{TD} \in \mathbb{R}^{n_{TD} \times 1}$ . For a lumped mass structural model with  $n$  floors, the state vector of the structure

dynamics,  $\mathbf{x}_S$ , consists of the relative displacement  $q_i$  and relative velocity  $\dot{q}_i$  (with respect to the ground) for each floor  $i$ ,  $i = 1, \dots, n$ .

$$\mathbf{x}_S = [q_1 \quad \dot{q}_1 \quad q_2 \quad \dot{q}_2 \quad \dots \quad q_n \quad \dot{q}_n]^T \quad (2)$$

The matrices  $\mathbf{A} \in \mathbb{R}^{n_{OL} \times n_{OL}}$ ,  $\mathbf{B}_1 \in \mathbb{R}^{n_{OL} \times n_w}$ , and  $\mathbf{B}_2 \in \mathbb{R}^{n_{OL} \times n_u}$  are, respectively, the discrete-time dynamics, excitation influence, and control influence matrices. The vector  $\mathbf{z} \in \mathbb{R}^{n_z \times 1}$  represents the response output (to be controlled using the feedback loop), and  $\mathbf{y} \in \mathbb{R}^{n_y \times 1}$  represents the time-delayed and noisy sensor measurement vector. Correspondingly, the matrices  $\mathbf{C}_1$ ,  $\mathbf{D}_{11}$ , and  $\mathbf{D}_{12}$  are termed the output parameter matrices, and the matrices  $\mathbf{C}_2$ ,  $\mathbf{D}_{21}$ , and  $\mathbf{D}_{22}$  are the measurement parameter matrices. In Eq. (1), time delay of one sampling period  $\Delta T$  is assumed for the sensor measurement signal (e.g. due to computational and/or communication latency). The formulation of the time-delay system can easily be extended to model multiple time delay steps, as well as different time delays for different sensors. Furthermore, the formulation can also represent fully decentralized control architecture, as well as information overlapping in a partially decentralized control architecture. Detailed description about the formulation can be found in Wang (2010).

Figure 1 summarizes the multiple components of the closed-loop control system. As shown in the figure, the open-loop system formulated in Eq. (1) contains the structural system and the system describing time delay, noise, and possible signal repeating. Output of the structural system, i.e. sensor measurement, is an input to the time-delay system. For the overall open-loop system, the inputs include the excitation  $\mathbf{w}_1[k]$ , the sensor noises  $\mathbf{w}_2[k]$ , and the control forces  $\mathbf{u}[k]$ ; outputs of the open-loop system include the structural response  $\mathbf{z}[k]$  and the feedback signals  $\mathbf{y}[k]$ . To complete the feedback control loop, the controller system takes the signal  $\mathbf{y}[k]$  as input and outputs the desired (optimal) control force vector  $\mathbf{u}[k]$  according to the following state-space equations:

$$\begin{cases} \mathbf{x}_G[k+1] = \mathbf{A}_G \mathbf{x}_G[k] + \mathbf{B}_G \mathbf{y}[k] \\ \mathbf{u}[k] = \mathbf{C}_G \mathbf{x}_G[k] + \mathbf{D}_G \mathbf{y}[k] \end{cases} \quad (3)$$

where  $\mathbf{A}_G$ ,  $\mathbf{B}_G$ ,  $\mathbf{C}_G$  and  $\mathbf{D}_G$  are the parametric matrices of the controller to be computed and, for

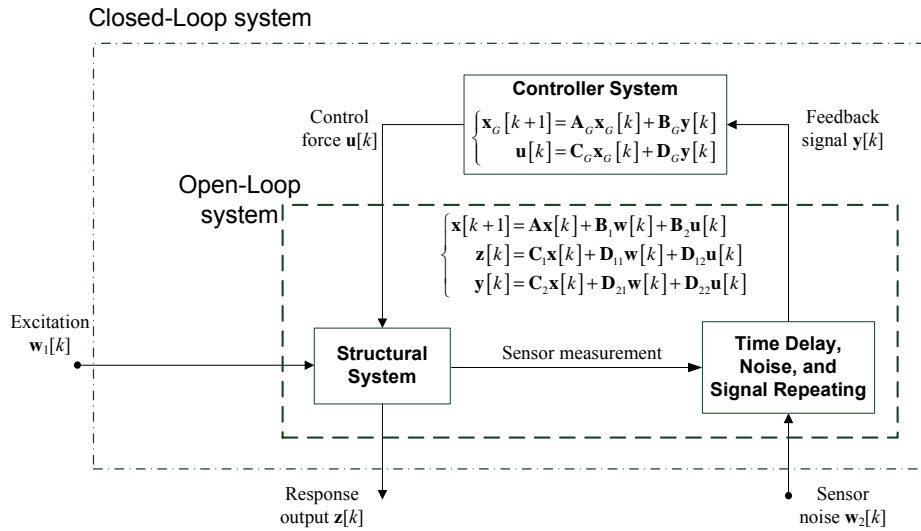


Figure 1. Diagram of the closed-loop control system.

convenience, are often collectively denoted by a controller matrix  $\mathbf{G} \in \mathbb{R}^{(n_G+n_u) \times (n_G+n_y)}$  as:

$$\mathbf{G} = \begin{bmatrix} \mathbf{A}_G & \mathbf{B}_G \\ \mathbf{C}_G & \mathbf{D}_G \end{bmatrix} \quad (4)$$

In this study, we assume the controller and the open-loop system have the same number of state variables, i.e.  $\mathbf{A}_G \in \mathbb{R}^{n_G \times n_G}$  and:

$$n_G = n_{OL} \quad (5)$$

### Decentralized Discrete-time $\mathcal{H}_2$ Controller Design

For decentralized control design, the feedback signals  $\mathbf{y}[k]$  and the control forces  $\mathbf{u}[k]$  are divided into  $N$  groups. For determining each group of control force, only one group of corresponding feedback signals is needed. To achieve this decentralized feedback pattern, the controller matrices can be specified to be block diagonal:

$$\mathbf{A}_G = \text{diag}(\mathbf{A}_{G_I}, \mathbf{A}_{G_{II}}, \dots, \mathbf{A}_{G_N}) \quad (6a)$$

$$\mathbf{B}_G = \text{diag}(\mathbf{B}_{G_I}, \mathbf{B}_{G_{II}}, \dots, \mathbf{B}_{G_N}) \quad (6b)$$

$$\mathbf{C}_G = \text{diag}(\mathbf{C}_{G_I}, \mathbf{C}_{G_{II}}, \dots, \mathbf{C}_{G_N}) \quad (6c)$$

$$\mathbf{D}_G = \text{diag}(\mathbf{D}_{G_I}, \mathbf{D}_{G_{II}}, \dots, \mathbf{D}_{G_N}) \quad (6d)$$

The control system in Eq. (3) is thus equivalent to a set of uncoupled decentralized controllers  $\mathbf{G}_i$  ( $i = I, II, \dots, N$ ):

$$\mathbf{G}_i = \begin{bmatrix} \mathbf{A}_{G_i} & \mathbf{B}_{G_i} \\ \mathbf{C}_{G_i} & \mathbf{D}_{G_i} \end{bmatrix} \quad (7)$$

Each controller  $\mathbf{G}_i$  requires only one group of feedback signals to determine the desired (optimal) control forces for one group of control devices:

$$\begin{cases} \mathbf{x}_{G_i}[k+1] = \mathbf{A}_{G_i} \mathbf{x}_{G_i}[k] + \mathbf{B}_{G_i} \mathbf{y}_i[k] \\ \mathbf{u}_i[k] = \mathbf{C}_{G_i} \mathbf{x}_{G_i}[k] + \mathbf{D}_{G_i} \mathbf{y}_i[k] \end{cases} \quad (8)$$

Assuming that the  $\mathbf{D}_{22}$  matrix in the open-loop system in Eq. (1) is a zero matrix, following notations are defined:

$$\left[ \begin{array}{c|c|c} \tilde{\mathbf{A}} & \tilde{\mathbf{B}}_1 & \tilde{\mathbf{B}}_2 \\ \hline \tilde{\mathbf{C}}_1 & \tilde{\mathbf{D}}_{11} & \tilde{\mathbf{D}}_{12} \\ \hline \tilde{\mathbf{C}}_2 & \tilde{\mathbf{D}}_{21} & \end{array} \right] = \left[ \begin{array}{cc|cc|c} \mathbf{A} & \mathbf{0} & \mathbf{B}_1 & \mathbf{0} & \mathbf{B}_2 \\ \mathbf{0} & \mathbf{0}_{n_G} & \mathbf{0} & \mathbf{I}_{n_G} & \mathbf{0} \\ \hline \mathbf{C}_1 & \mathbf{0} & \mathbf{D}_{11} & \mathbf{0} & \mathbf{D}_{12} \\ \hline \mathbf{0} & \mathbf{I}_{n_G} & \mathbf{0} & & \\ \mathbf{C}_2 & \mathbf{0} & \mathbf{D}_{21} & & \end{array} \right] \quad (9)$$

Zero submatrices with unspecified dimensions should have compatible dimensions with neighboring submatrices. Using the definitions above, the closed-loop system can be formulated by concatenating the open-loop system in Eq. (1) with the controller system in Eq. (3):

$$\begin{cases} \mathbf{x}_{CL}[k+1] = \mathbf{A}_{CL}\mathbf{x}_{CL}[k] + \mathbf{B}_{CL}\mathbf{w}[k] \\ \mathbf{z}[k] = \mathbf{C}_{CL}\mathbf{x}_{CL}[k] + \mathbf{D}_{CL}\mathbf{w}[k] \end{cases} \quad (10)$$

where

$$\mathbf{A}_{CL} = \tilde{\mathbf{A}} + \tilde{\mathbf{B}}_2\mathbf{G}\tilde{\mathbf{C}}_2 \quad (11a)$$

$$\mathbf{B}_{CL} = \tilde{\mathbf{B}}_1 + \tilde{\mathbf{B}}_2\mathbf{G}\tilde{\mathbf{D}}_{21} \quad (11b)$$

$$\mathbf{C}_{CL} = \tilde{\mathbf{C}}_1 + \tilde{\mathbf{D}}_{12}\mathbf{G}\tilde{\mathbf{C}}_2 \quad (11c)$$

$$\mathbf{D}_{CL} = \tilde{\mathbf{D}}_{11} + \tilde{\mathbf{D}}_{12}\mathbf{G}\tilde{\mathbf{D}}_{21} \quad (11d)$$

and  $\mathbf{G}$  is as defined in Eq. (4). Note that the input to the closed-loop system is  $\mathbf{w}[k]$ , which contains the external excitation  $\mathbf{w}_1[k]$  and sensor noises  $\mathbf{w}_2[k]$ , while the output is same as the structural output  $\mathbf{z}[k]$  defined in Eq. (1). Using Z-transform (Franklin *et al.* 1998), the dynamics of a discrete-time system can be represented by the transfer function  $\mathbf{H}_{zw}(z) \in \mathbb{C}^{n_z \times n_w}$  from disturbance  $\mathbf{w}$  to output  $\mathbf{z}$  as:

$$\mathbf{H}_{zw}(z) = \mathbf{C}_{CL}(z\mathbf{I} - \mathbf{A}_{CL})^{-1}\mathbf{B}_{CL} + \mathbf{D}_{CL} \quad (12)$$

The objective of  $\mathcal{H}_2$  control is to minimize the  $\mathcal{H}_2$ -norm of the closed-loop discrete-time system, which in the frequency domain is defined as:

$$\|\mathbf{H}_{zw}\|_2 = \sqrt{\frac{\Delta T}{2\pi} \int_{-\omega_N}^{+\omega_N} \text{Trace}\{\mathbf{H}_{zw}^*(e^{j\omega\Delta T})\mathbf{H}_{zw}(e^{j\omega\Delta T})\}d\omega} \quad (13)$$

where  $\omega$  represents angular frequency,  $\omega_N = \pi/\Delta T$  is the Nyquist frequency,  $j$  is the imaginary unit,  $\mathbf{H}_{zw}^*$  is the complex conjugate transpose of  $\mathbf{H}_{zw}$ , and  $\text{Trace}\{\cdot\}$  denotes the trace of a square matrix.

It has been well established that the  $\mathcal{H}_2$ -norm of the closed-loop system in Eq. (10) is less than a positive number  $\gamma$ , if, and only if, there exist symmetric positive definite matrices  $\mathbf{P}$  and  $\mathbf{R}$  such that the following inequalities holds (Masubuchi *et al.* 1998; Paganini and Feron 2000):

$$\begin{bmatrix} \mathbf{P} & \mathbf{P}\mathbf{A}_{CL} & \mathbf{P}\mathbf{B}_{CL} \\ * & \mathbf{P} & \mathbf{0} \\ * & * & \mathbf{I} \end{bmatrix} > 0 \quad (14a)$$

$$\begin{bmatrix} \mathbf{R} & \mathbf{C}_{CL} & \mathbf{D}_{CL} \\ * & \mathbf{P} & \mathbf{0} \\ * & * & \mathbf{I} \end{bmatrix} > 0 \quad (14b)$$

$$\text{Trace}(\mathbf{R}) < \gamma \quad (14c)$$

where \* denotes a symmetric entry; “> 0” means that the matrix at the left side of the inequality is positive definite.

Substituting the definitions in Eq. (11) into the left side of Eqs. (14a) and (14b), the matrix variable  $\mathbf{F}_1$  is now defined as a function of  $\mathbf{G}$  and  $\mathbf{P}$ , and the matrix variable  $\mathbf{F}_2$  as a function of  $\mathbf{G}$ ,  $\mathbf{P}$ , and  $\mathbf{R}$ :

$$\mathbf{F}_1(\mathbf{G}, \mathbf{P}) = \begin{bmatrix} \mathbf{P} & \mathbf{P}(\tilde{\mathbf{A}} + \tilde{\mathbf{B}}_2\mathbf{G}\tilde{\mathbf{C}}_2) & \mathbf{P}(\tilde{\mathbf{B}}_1 + \tilde{\mathbf{B}}_2\mathbf{G}\tilde{\mathbf{D}}_{21}) \\ * & \mathbf{P} & \mathbf{0} \\ * & * & \mathbf{I} \end{bmatrix} \quad (15a)$$

$$\mathbf{F}_2(\mathbf{G}, \mathbf{P}, \mathbf{R}) = \begin{bmatrix} \mathbf{R} & \tilde{\mathbf{C}}_1 + \tilde{\mathbf{D}}_{12}\mathbf{G}\tilde{\mathbf{C}}_2 & \tilde{\mathbf{D}}_{11} + \tilde{\mathbf{D}}_{12}\mathbf{G}\tilde{\mathbf{D}}_{21} \\ * & \mathbf{P} & \mathbf{0} \\ * & * & \mathbf{I} \end{bmatrix} \quad (15b)$$

In summary, the closed-loop  $\mathcal{H}_2$ -norm is less than  $\gamma$  if there exist symmetric positive definite matrices  $\mathbf{P}$  and  $\mathbf{R}$  such that

$$\mathbf{F}_1(\mathbf{G}, \mathbf{P}) > 0, \mathbf{F}_2(\mathbf{G}, \mathbf{P}, \mathbf{R}) > 0, \text{ and } \text{Trace}(\mathbf{R}) < \gamma \quad (16)$$

For a decentralized control solution, the  $\mathcal{H}_2$ -norm criteria  $\|\mathbf{H}_{zw}\|_2 < \gamma$  is satisfied if a decentralized controller matrix  $\mathbf{G}$  (with parametric structures illustrated in Eq. (10)), together with symmetric positive definite matrices  $\mathbf{P}$  and  $\mathbf{R}$ , can be found so that the three inequalities in Eq. (16) are satisfied. Because both  $\mathbf{G}$  and  $\mathbf{P}$  are unknown variables, the problem has a bilinear matrix inequality (BMI) constraint (VanAntwerp and Braatz 2000) as specified in Eq. (15).

When there is no sparsity requirement on matrix  $\mathbf{G}$ , efficient algorithms and solvers are available for computing an ordinary controller matrix  $\mathbf{G}_c$  that minimizes the closed-loop  $\mathcal{H}_2$ -norm (Chiang and Safonov 1998; Doyle *et al.* 1989):

$$\mathbf{G}_c = \begin{bmatrix} \mathbf{A}_{G_c} & \mathbf{B}_{G_c} \\ \mathbf{C}_{G_c} & \mathbf{D}_{G_c} \end{bmatrix} \quad (17)$$

In general,  $\mathbf{A}_{G_c}$ ,  $\mathbf{B}_{G_c}$ ,  $\mathbf{C}_{G_c}$ , and  $\mathbf{D}_{G_c}$  are full matrices that represent centralized information feedback. When sparsity patterns (such as block-diagonal forms) in the controller parametric matrices are specified to achieve decentralized information feedback, off-the-shelf algorithms or numerical packages for solving the optimization problem with BMI constraints are not available (Goh *et al.* 1994; VanAntwerp and Braatz 2000). A heuristic homotopy method for designing continuous-time decentralized  $\mathcal{H}_\infty$  controllers, which was described by Zhai, *et al.* (2001), is adapted for the discrete-time  $\mathcal{H}_2$  controller design in this study. Starting with a centralized controller, the homotopy method gradually transforms the controller into a decentralized one. The algorithm searches for a decentralized controller along the following homotopy path:

$$\mathbf{G} = (1 - \lambda)\mathbf{G}_C + \lambda\mathbf{G}_D, 0 \leq \lambda \leq 1 \quad (18)$$

where  $\lambda$  gradually increases from 0 to 1.  $\mathbf{G}_C$  represents the initial centralized controller to start with and  $\mathbf{G}_D$  represents the desired decentralized controller with the sparsity pattern shown in Eq. (10). For a total number of  $M$  steps assigned for the homotopy path, the increment is specified as:

$$\lambda_k = k/M, k = 0, 1, \dots, M \quad (19)$$

At every step  $k$  along the homotopy path, the two matrix variables  $\mathbf{G}_D$  and  $\mathbf{P}$  are held constant one at a time, so that only one of them needs to be solved at each time. In this way, the BMI constraint in Eq. (15) degenerates into a linear matrix inequality (LMI) constraint. For convenience, matrix variables  $\mathbf{V}_1$  and  $\mathbf{V}_2$  are defined based on Eqs. (15a) and (15b):

$$\mathbf{V}_1(\mathbf{G}_D, \mathbf{P}, \lambda) = \mathbf{F}_1(\mathbf{G}, \mathbf{P}) = \mathbf{F}_1((1 - \lambda)\mathbf{G}_C + \lambda\mathbf{G}_D, \mathbf{P}) \quad (20a)$$

$$\mathbf{V}_2(\mathbf{G}_D, \mathbf{P}, \lambda, \mathbf{R}) = \mathbf{F}_2(\mathbf{G}, \mathbf{P}, \mathbf{R}) = \mathbf{F}_2((1 - \lambda)\mathbf{G}_C + \lambda\mathbf{G}_D, \mathbf{P}, \mathbf{R}) \quad (20b)$$

Note that the centralized controller  $\mathbf{G}_C$  is initially solved using conventional methods and remains constant during the homotopy search. At the beginning of every homotopy search, an upper bound for the closed-loop  $\mathcal{H}_2$ -norm, *i.e.*  $\gamma$  is specified. When  $\mathbf{G}_D$  is held constant, a new  $\mathbf{P}$  matrix (together with a new  $\mathbf{R}$  matrix) can be computed for the next homotopy step, under the LMI constraints; on the other hand, when  $\mathbf{P}$  is held constant, a new  $\mathbf{G}_D$  matrix (together with a new  $\mathbf{R}$  matrix) is computed under the LMI constraints. If a homotopy search fails,  $\gamma$  is increased by certain relaxation factor and a new search is conducted. The overall algorithm can be described as follows:

- [i] Compute a centralized controller  $\mathbf{G}_C$  and the minimum closed-loop  $\mathcal{H}_2$ -norm  $\gamma_C$  using existing robust control solvers (Chiang and Safonov 1998; Doyle *et al.* 1989); set  $\gamma \leftarrow \gamma_C$ , and set an upper limit ( $\gamma_{\max}$ ) for  $\gamma$  e.g.  $10^6 \gamma_C$ .
- [ii] Initialize  $M$ , the total number of homotopy steps, to be a positive number, e.g.  $2^8$ , and set an upper limit ( $M_{\max}$ ) for  $M$ , e.g.  $2^{13}$ ; Set  $k \leftarrow 0$ ,  $\lambda_0 \leftarrow 0$ , and  $\mathbf{G}_{D0} \leftarrow \mathbf{0}$ ; compute a feasible solution for  $\mathbf{P}_0$  and  $\mathbf{R}$  under following LMI constraints:

$$\mathbf{V}_1(\mathbf{G}_{D0}, \mathbf{P}_0, \lambda_0) > 0, \quad \mathbf{V}_2(\mathbf{G}_{D0}, \mathbf{P}_0, \lambda_0, \mathbf{R}) > 0, \quad \text{and} \quad \text{Trace}(\mathbf{R}) < \gamma \quad (21)$$

[iii] Set  $k \leftarrow k+1$ , and  $\lambda_k \leftarrow k/M$ ; compute  $\mathbf{G}_D$  and  $\mathbf{R}$  under following LMI constraints:

$$\mathbf{V}_1(\mathbf{G}_D, \mathbf{P}_{k-1}, \lambda_k) > 0, \quad \mathbf{V}_2(\mathbf{G}_D, \mathbf{P}_{k-1}, \lambda_k, \mathbf{R}) > 0, \quad \text{and} \quad \text{Trace}(\mathbf{R}) < \gamma \quad (22)$$

If the solution is not feasible, go to Step [iv]. If the solution is feasible, set  $\mathbf{G}_{Dk} \leftarrow \mathbf{G}_D$ , and compute  $\mathbf{P}$  and  $\mathbf{R}$  under LMI constraints:

$$\mathbf{V}_1(\mathbf{G}_{Dk}, \mathbf{P}, \lambda_k) > 0, \quad \mathbf{V}_2(\mathbf{G}_{Dk}, \mathbf{P}, \lambda_k, \mathbf{R}) > 0, \quad \text{and} \quad \text{Trace}(\mathbf{R}) < \gamma \quad (23)$$

If the solution is feasible, set  $\mathbf{P}_k \leftarrow \mathbf{P}$ , and go to Step [v]; if not, go to Step [vi].

[iv] Compute  $\mathbf{P}$  and  $\mathbf{R}$  under LMI constraints:

$$\mathbf{V}_1(\mathbf{G}_{D_{k-1}}, \mathbf{P}, \lambda_k) > 0, \quad \mathbf{V}_2(\mathbf{G}_{D_{k-1}}, \mathbf{P}, \lambda_k, \mathbf{R}) > 0, \quad \text{and} \quad \text{Trace}(\mathbf{R}) < \gamma \quad (24)$$

If the solution is not feasible, go to Step [vi]. If it is feasible, set  $\mathbf{P}_k \leftarrow \mathbf{P}$  and compute  $\mathbf{G}_D$  and  $\mathbf{R}$  under the LMI constraints:

$$\mathbf{V}_1(\mathbf{G}_D, \mathbf{P}_k, \lambda_k) > 0, \quad \mathbf{V}_2(\mathbf{G}_D, \mathbf{P}_k, \lambda_k, \mathbf{R}) > 0, \quad \text{and} \quad \text{Trace}(\mathbf{R}) < \gamma \quad (25)$$

If the solution is feasible, set  $\mathbf{G}_{Dk} \leftarrow \mathbf{G}_D$  and go to Step [v]; if not, go to Step [vi].

[v] If  $k < M$ , go to Step [iii]. If  $k$  is equal to  $M$ ,  $\mathbf{G}_{Dk}$  is the solution of the decentralized control problem, and the search ends here.

[vi] Set  $M \leftarrow 2M$  under the constraint  $M \leq M_{\max}$  and restart the searching from Step [ii]. If  $M$  reaches beyond  $M_{\max}$ , set  $\gamma \leftarrow s_\gamma \gamma$  ( $s_\gamma$  is a relaxation factor that is greater than one) under the constraint  $\gamma \leq \gamma_{\max}$  and restart from Step [ii]. If  $\gamma$  exceeds  $\gamma_{\max}$ , it is concluded that the computation doesn't converge.

A decentralized controller is found when  $k$  reaches  $M$  at step [v]. The controller has the property that the closed-loop  $\mathcal{H}_2$ -norm is less than  $\gamma$ . It should be pointed out that since the homotopy method is heuristic in nature, non-convergence in the computation does not imply that the decentralized  $\mathcal{H}_2$  control problem has no solution.

## Numerical Example

This section first illustrates procedures of the decentralized  $\mathcal{H}_2$  controller design using a five-story example structure. Simulations are conducted to demonstrate the performance of different decentralized and centralized feedback architectures. Performance of the  $\mathcal{H}_2$  controllers is compared with the performance of time-delayed controllers that are based on  $\mathcal{H}_\infty$  control criteria or linear quadratic regulator (LQR) criteria.

### Formulation of the five-story example structure

A five-story model similar to the Kajima-Shizuoka Building is employed (Kurata *et al.* 1999). The five-story building is modeled as an in-plane lumped-mass structure with control devices allocated between every two neighboring floors. Details about the simulation model can be found in Wang (2010), where the formulation of the discrete-time structural control system is described as well. In short, the system output matrices,  $\mathbf{C}_1$ ,  $\mathbf{D}_{11}$ , and  $\mathbf{D}_{12}$  in Eq. (1), are defined so that the output vector contains both structural response and control effort:

$$\mathbf{z} = \begin{Bmatrix} \mathbf{z}_1 \\ \mathbf{z}_2 \end{Bmatrix} \quad (26)$$

where sub-vector  $\mathbf{z}_1$  contains entries related to the inter-story drift response at all stories, and sub-vector  $\mathbf{z}_2$  contains entries related to control forces. The relative weighting between the structural response and the control effort is reflected by the magnitude of the output matrices. With regard to feedback sensor data, it is assumed that inter-story drifts and velocities can be measured.

### Controller design with different feedback control architectures

As illustrated in Figure 2, different control feedback architectures are designed for different degrees of centralization (DC), which denote the number of neighboring floors that constitute a communication subnet and share their sensor data. In each feedback architecture, one or more communication subnets exist, with each communication subnet (as denoted by channels Ch1, Ch2, etc.) covering a limited number of stories. The controllers covered by a subnet are allowed to access the sensor data within that subnet. For DC5, one subnet covers all five floors, which results in a centralized information architecture. Figure 2 also demonstrates the story coverage of each (de)centralized controller, such as  $\mathbf{G}_I$ ,  $\mathbf{G}_{II}$ , etc, for every control architecture. All control devices in one story should be commanded by the controller covering this story, which guarantees that a control device can only be commanded by one controller. For stories that belong to multiple overlapping subnets (such as in cases DC2, DC3, and DC4), each controller at these stories should have communication access to data within all the overlapping subnets. For example, for case DC2, controller  $\mathbf{G}_{II}$  obtains data from sensors at the 1<sup>st</sup> and the 2<sup>nd</sup> story through communication subnet Ch1, as well as data at the 3<sup>rd</sup> story through communication subnet Ch2.

Table 1 lists the dimensions of the all (de)centralized controllers for each control architecture. For case DC1, each decentralized controller takes two feedback signals as input (*i.e.* inter-story drift and velocity at the story covered by the controller), and outputs the desired control force at this story. For the partially decentralized case DC2, the input for each controller contains sensor data that are obtained through

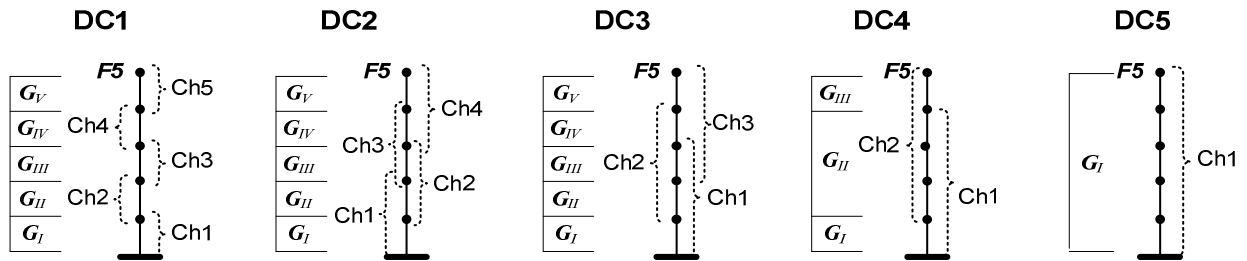


**Figure 2. Communication subnet partitioning for different degrees of centralization (DC) applied to the five-story simulation model.**

multiple communication subnets. For example, controller  $\mathbf{G}_{II}$  in case DC2 has access to inter-story drift and velocity data from the 1<sup>st</sup>, 2<sup>nd</sup>, and 3<sup>rd</sup> stories, which lead to six input variables. The number of input variables for other control architectures can be determined in a similar fashion. In addition, Table 1 shows that all five control architectures have the same total number of state variables,  $n_G = 20$ , which is equal to the number of state variables of the open loop system,  $n_{OL}$  (as described in Eq. (5)). All five control architectures also have the same total number of output variables, which correspond to the control forces at the five stories.

**Table 1 Dimensions of the (de)centralized dynamic controllers for each control architecture**

	DC1					DC2					DC3					DC4			DC5
	$G_I$	$G_{II}$	$G_{III}$	$G_{IV}$	$G_V$	$G_I$	$G_{II}$	$G_{III}$	$G_{IV}$	$G_V$	$G_I$	$G_{II}$	$G_{III}$	$G_{IV}$	$G_V$	$G_I$	$G_{II}$	$G_{III}$	$G_I$
Input	2	2	2	2	2	4	6	6	6	4	6	8	10	8	6	8	10	8	10
State	4	4	4	4	4	4	4	4	4	4	4	4	4	4	4	4	12	4	20
Output	1	1	1	1	1	1	1	1	1	1	1	1	1	1	1	1	3	1	5

A sampling period of 5 ms is first used for all (de)centralized feedback architectures; this implies that the feedback time delay is also set as 5 ms. Table 2 lists the open-loop  $\mathcal{H}_2$ -norm  $\|\mathbf{H}_{zw}\|_2$  of the uncontrolled structure, as well as the closed-loop  $\mathcal{H}_2$ -norms using different control architectures. The  $\mathcal{H}_2$ -norm of the uncontrolled structure is computed by neglecting the control force and sensor measurement in the formulation. With 5ms of time delay existing in the feedback loop, all controllers show stable performance and achieve smaller  $\mathcal{H}_2$ -norm than the uncontrolled case. Among the control cases, the centralized controller (case DC5) achieves minimum closed-loop  $\mathcal{H}_2$ -norm (which means “best” control performance), which is because case DC5 has the most complete sensor data available for the control decisions for all five control devices. In general, the higher the degree of centralization is, the smaller  $\|\mathbf{H}_{zw}\|_2$  becomes; although the exception is that cases DC3 and DC4 have larger closed-loop  $\mathcal{H}_2$ -norms than case DC2. Such irregularity can be attributed to the non-convexity nature of the optimal decentralized control problem, and the fact that the homotopy transformation algorithm is heuristic and cannot guarantee global optimum.

**Table 2  $\mathcal{H}_2$ -norms of controlled (with 5ms feedback time delay) and uncontrolled structures**

	Uncontrolled	DC1	DC2	DC3	DC4	DC5 (centralized)
$\ \mathbf{H}_{zw}\ _2$	5.94	4.47	4.35	5.13	4.47	4.18

*Simulation results of decentralized and centralized  $\mathcal{H}_2$  control*

In this simulation study, the 1995 Kobe NS (JMA Station) earthquake record with its peak acceleration scaled to  $1\text{m/s}^2$  is used as the ground excitation. Ideal actuators that generate any desired control forces are deployed at the five stories. In practical implementation, longer communication and computation time delays may be induced as the control architecture becomes more centralized. In order to illustrate the effect of such varying time delays, simulations are conducted with different time delays adopted for

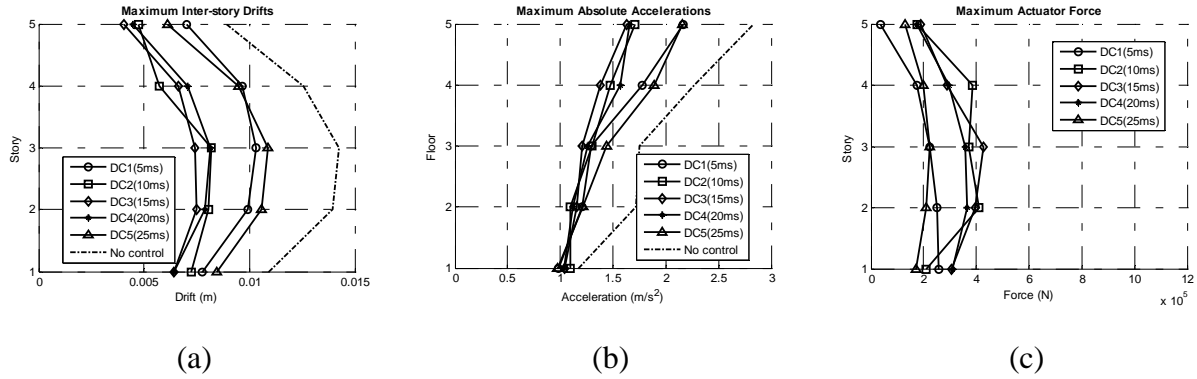


**Figure 3. Simulation results for  $\mathcal{H}_2$  control with different time delays: (a) peak inter-story drifts; (b) peak absolute accelerations; (c) peak control forces.**

the five different control architectures. For case DC1, where each controller only requires sensor data at its own story to make control decisions, time delay is chosen to be the minimum of 5ms. For case DC2, where data from sensors on a control device's own story and neighboring story (stories) are required, time delay is chosen as 10ms. Similarly, for the cases DC3, DC4, and DC5, where more sensor data need to be communicated and processed, time delay of 15ms, 20ms, and 25ms are assigned, respectively.

Using the newly computed controllers based on different time delays, Figure 3 presents the peak values of the inter-story drifts, absolute accelerations, and actuator forces at each story (floor). Compared with the uncontrolled case, all five controlled cases achieve significant reduction to structural response, and demonstrate stability with different amount of time delays in the feedback loop. The fully decentralized case without any information overlapping, case DC1, achieves similar reduction to inter-story drifts along all stories while compared with the centralized case DC5. Meanwhile, case DC1 achieves similar reduction to peak floor accelerations and requires similar peak actuator forces as case DC5. Other partially decentralized cases with information overlapping, including DC2, DC3, and DC4, generally achieve more reduction to the peak drifts, while at the expense of larger peak control forces.

Figure 4 presents the root-mean-square (RMS) values of the inter-story drifts, absolute accelerations, and actuator forces at each story (floor). Again, when comparing with the uncontrolled structure, significant

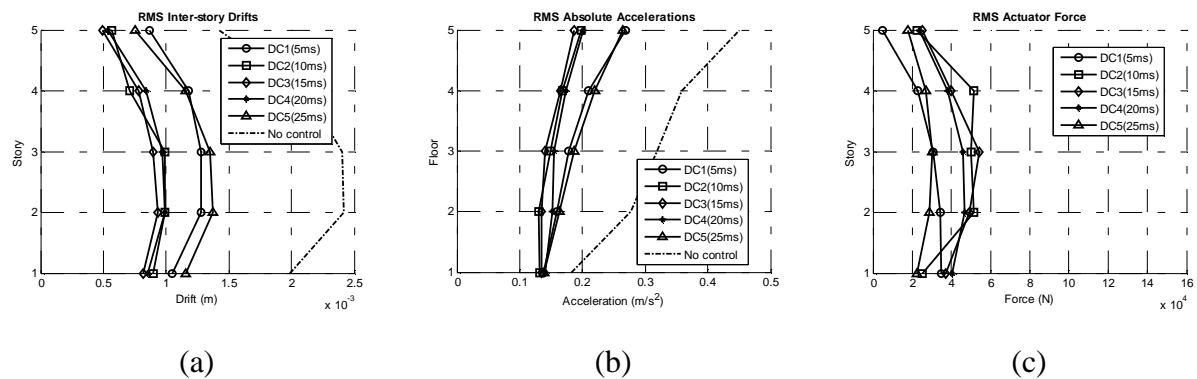


**Figure 4. Simulation results for  $\mathcal{H}_2$  control with different time delays: (a) RMS inter-story drifts; (b) RMS absolute accelerations; (c) RMS control forces (note that the horizontal scales are different from these in Figure 3).**

reduction to inter-story drifts and floor accelerations are achieved for all the control cases with feedback time delay. Similar to the peak value plots in Figure 3, Figure 4 shows that in general, cases DC2, DC3, and DC4, achieve more reduction to RMS inter-story drifts at the expense of larger control effort. Nevertheless, it is demonstrated that the decentralized  $\mathcal{H}_2$  controllers are able to provide reasonable control performance with various time delays existing in the feedback loop.

In addition, the performance results for the  $\mathcal{H}_2$  controller design as shown in Figures 3 and 4 can be used to compare with the simulation results of time-delayed (de)centralized LQR controllers and  $\mathcal{H}_\infty$  controllers previously presented in Wang (2010). Generally speaking, the performance of the  $\mathcal{H}_2$  controllers lies between the LQR and the  $\mathcal{H}_\infty$  controllers. Specifically, for each control architecture, the (de)centralized  $\mathcal{H}_2$  controller usually achieves less reduction in structural response than the  $\mathcal{H}_\infty$  controller, but more reduction than the LQR controller. On the other hand, the  $\mathcal{H}_2$  controller usually consumes less control efforts than the  $\mathcal{H}_\infty$  controller, but more control effort than the LQR controller.

For practical applications of feedback structural control, one of the major constraints is the realistic capacity of the semi-active or active control devices. Total actuator capacity (i.e. the sum of the force capacities of all control devices installed in the structure) is usually adopted as an indicator to quantify the force capacity requirements of a structural control system. As suggested by many references on building structure control, it is realistic to have the percentage of the total actuator capacity over building weight to be around 10% ~ 20% (Barroso *et al.* 2003; Kannan *et al.* 1995; Kim and Jabbari 2002). The average total actuator capacity among five (de)centralized control architectures is calculated for the three different controller designs, including  $\mathcal{H}_2$  control, LQR control, and  $\mathcal{H}_\infty$  control. For the three different controller designs, Table 3 lists the total actuator capacities and their percentages over the weight of the entire five-story building, which is about 10,803kN. It can be seen that in this numerical simulation, the actuator capacity required by the  $\mathcal{H}_\infty$  control is slightly higher than the realistic range, which may cause difficulty in practical applications. On the other hand, the total actuator capacity required by LQR control is lower than the realistic range, which suggests that in this example, the LQR controller design may not be able to make the best utilization of the full capacity of realistic actuators. Among the three controller designs, the  $\mathcal{H}_2$  controller design has realistic requirement on total actuator capacity, and shows good utilization of the actuator capacity for adequate control performance.

**Table 3 Total actuator capacity requirement of three controller designs**

	LQR	$\mathcal{H}_2$	$\mathcal{H}_\infty$
Total actuator capacity	793 kN	1306 kN	2339 kN
Percentage over building weight	7.3%	12.1%	21.7%

## Summary and Conclusion

This paper presents a decentralized control approach that aims to minimize the closed-loop  $\mathcal{H}_2$  norm of a controlled civil structure. The approach is formulated in discrete-time domain, and considers possible feedback time delay. The heuristic decentralized controller design employs a homotopy method, which gradually transforms an original centralized controller into uncoupled decentralized ones. Through a five-story example, it was identified that using similar parameters in the problem formulation, the  $\mathcal{H}_2$  controller design may achieve agreeable performance without excessive requirement on actuator capacity.

Nevertheless, it should be noted that the homotopy approach for decentralized  $\mathcal{H}_2$  controller design is heuristic. The approach may not guarantee the minimum  $\mathcal{H}_2$ -norm over the complete solution space. Since the proposed controller design is based on the assumption of system linearity, further study is needed on improving the control performance with non-linear control devices. Shake-table experiments are being planned to further examine the performance of the decentralized  $\mathcal{H}_2$  controller design, particularly in comparison with decentralized LQR and  $\mathcal{H}_\infty$  controller designs.

### Acknowledgement

The author appreciates the insightful opinions to this study provided by Prof. Sanjay Lall of the Department of Aeronautics and Astronautics at Stanford University. This research is partially funded by an NSF grant CMMI 0824977 awarded to Prof. Kincho H. Law at Stanford University. Any opinions and findings are those of the authors, and do not necessarily reflect the views of NSF or their collaborators.

### References

- Ankireddi, S., and H. T. Y. Yang. (1999). "Sampled-data  $H_2$  optimal output feedback control for civil structures." *Earthquake Engineering & Structural Dynamics*, 28(9), 921-940.
- Barroso, L. R., J. G. Chase, and S. Hunt. (2003). "Resettable smart dampers for multi-level seismic hazard mitigation of steel moment frames." *Journal of Structural Control*, 10(1), 41-58.
- Cao, D. Q., J. M. Ko, Y. Q. Ni, and H. J. Liu. (2000). "Decentralized active tendon control and stability of cable-stayed bridges." *Advances in Structural Dynamics*, 2, 1257-1264.
- Chiang, R. Y., and M. G. Safonov. (1998). *MATLAB robust control toolbox*, MathWorks, Inc., Natick, MA.
- Doyle, J. C., K. Glover, P. P. Khargonekar, and B. A. Francis. (1989). "State-space solutions to standard  $H_2$  and  $H_\infty$  control problems." *Automatic Control, IEEE Transactions on*, 34(8), 831-847.
- Dyke, S. J., B. F. Spencer, Jr., P. Quast, J. D. C. Kaspari, and M. K. Sain. (1996). "Implementation of an active mass driver using acceleration feedback control." *Computer-Aided Civil and Infrastructure Engineering*, 11(5), 305-323.
- Franklin, G. F., J. D. Powell, and M. L. Workman. (1998). *Digital Control of Dynamic Systems*, Addison-Wesley, Menlo Park, CA.
- Goh, K. C., M. G. Safonov, and G. P. Papavassilopoulos. (1994). "A global optimization approach for the BMI problem." *Proceedings of the 33rd IEEE Conference on Decision and Control*. Lake Buena Vista, FL, USA. December 14-16, 1994.
- Hiramoto, K., and K. Grigoriadis. (2008). "Upper bound  $H_\infty$  and  $H_2$  control for collocated structural systems." *Structural Control and Health Monitoring*, 16(4), 425 - 440.
- Housner, G. W., L. A. Bergman, T. K. Caughey, A. G. Chassiakos, R. O. Claus, S. F. Masri, R. E. Skelton, T. T. Soong, B. F. Spencer, Jr., and J. T. P. Yao. (1997). "Structural control: past, present, and future." *Journal of Engineering Mechanics*, 123(9), 897-971.
- Johnson, E. A., P. G. Voulgaris, and L. A. Bergman. (1998). "Multiobjective optimal structural control of the Notre Dame building model benchmark." *Earthquake Engineering & Structural Dynamics*, 27(11), 1165-1187.
- Kannan, S., H. M. Uras, and H. M. Aktan. (1995). "Active control of building seismic response by energy dissipation." *Earthquake Engineering & Structural Dynamics*, 24(5), 747-759.
- Kim, J.-H., and F. Jabbari. (2002). "Actuator saturation and control design for buildings under seismic excitation." *Journal of Engineering Mechanics*, 128(4), 403-412.
- Kurata, N., T. Kobori, M. Takahashi, N. Niwa, and H. Midorikawa. (1999). "Actual seismic response controlled building with semi-active damper system." *Earthquake Engineering & Structural Dynamics*, 28(11), 1427-1447.
- Loh, C.-H., and C.-M. Chang. (2008). "Application of centralized and decentralized control to building structure: analytical study." *Journal of Engineering Mechanics*, 134(11), 970-982.
- Lu, K.-C., C.-H. Loh, J. N. Yang, and P.-Y. Lin. (2008). "Decentralized sliding mode control of a building using MR dampers." *Smart Materials and Structures*, 17(5), 055006.
- Luo, N., J. Rodellar, M. de la Sen, and J. Vehí. (2002). "Decentralized active control of a class of uncertain cable-stayed flexible structures." *International Journal of Control*, 75(4), 285-296.
- Lynch, J. P., and K. H. Law. (2002). "Market-based control of linear structural systems." *Earthquake Engineering & Structural Dynamics*, 31(10), 1855-1877.

- Lynch, J. P., and K. H. Law. (2004). "Decentralized energy market-based structural control." *Structural Engineering and Mechanics*, 17(3-4), 557-572.
- Masubuchi, I., A. Ohara, and N. Suda. (1998). "LMI-based controller synthesis: A unified formulation and solution." *International Journal of Robust and Nonlinear Control*, 8(8), 669-686.
- Mehendale, C. S., and K. M. Grigoriadis. (2008). "A double homotopy method for decentralised control design." *International Journal of Control*, 81(10), 1600 - 1608.
- Paganini, F., and E. Feron. (2000). "Linear matrix inequality methods for robust  $H_2$  analysis: a survey with comparisons." *Advances in Linear Matrix Inequality Methods in Control: Advances in Design and Control*, L. E. Ghaoui and S.-I. Niculescu, eds., Society for Industrial and Applied Mathematics, 129-151.
- Sandell, N., Jr., P. Varaiya, M. Athans, and M. Safonov. (1978). "Survey of decentralized control methods for large scale systems." *Automatic Control, IEEE Transactions on*, 23(2), 108-128.
- Siljak, D. D. (1991). *Decentralized Control of Complex Systems*, Academic Press, Boston.
- Spencer, B. F., Jr., and S. Nagarajaiah. (2003). "State of the art of structural control." *Journal of Structural Engineering*, 129(7), 845-856.
- Spencer, B. F., Jr., J. Suhardjo, and M. K. Sain. (1994). "Frequency domain optimal control strategies for aseismic protection." *Journal of Engineering Mechanics*, 120(1), 135-158.
- Swartz, R. A., and J. P. Lynch. (2009). "Strategic network utilization in a wireless structural control system for seismically excited structures." *Journal of Structural Engineering*, 135(5), 597-608.
- VanAntwerp, J. G., and R. D. Braatz. (2000). "A tutorial on linear and bilinear matrix inequalities." *Journal of Process Control*, 10(4), 363-385.
- Volz, P., M. E. Magana, A. G. Henried, and T. H. Miller. (1994). "A decentralized active controller for cable-stayed bridges." *Proceedings of the 1st World Conference on Structural Control*. Los Angeles, CA. August 3 - 5 1994.
- Wang, Y. (2010). "Time-delayed dynamic output feedback  $H_\infty$  controller design for civil structures: a decentralized approach through homotopic transformation." *Structural Control and Health Monitoring*, <http://dx.doi.org/10.1002/stc.344> (in print).
- Wang, Y., K. H. Law, and S. Lall. (2009). "Time-delayed decentralized  $H_\infty$  controller design for civil structures: a homotopy method through linear matrix inequalities." *Proceedings of the 2009 American Control Conference (ACC 2009)*. St. Louis, MO, USA. June 10 - 12, 2009.
- Wang, Y., R. A. Swartz, J. P. Lynch, K. H. Law, K.-C. Lu, and C.-H. Loh. (2007). "Decentralized civil structural control using real-time wireless sensing and embedded computing." *Smart Structures and Systems*, 3(3), 321-340.
- Yang, J. N., S. Lin, and F. Jabbari. (2003). " $H_2$ -based control strategies for civil engineering structures." *Journal of Structural Control*, 10(3-4), 205-230.
- Zhai, G., M. Ikeda, and Y. Fujisaki. (2001). "Decentralized  $H_\infty$  controller design: a matrix inequality approach using a homotopy method." *Automatica*, 37(4), 565-572.